



# Replacement of eggs with soybean protein isolates and polysaccharides to prepare yellow cakes suitable for vegetarians



Muyang Lin<sup>a,b</sup>, Siang Hong Tay<sup>a</sup>, Hongshun Yang<sup>a,b,\*</sup>, Bao Yang<sup>c</sup>, Hongliang Li<sup>d</sup>

<sup>a</sup> Food Science and Technology Programme, c/o Department of Chemistry, National University of Singapore, Singapore 117543, Republic of Singapore

<sup>b</sup> National University of Singapore (Suzhou) Research Institute, 377 Lin Qian Street, Suzhou Industrial Park, Suzhou, Jiangsu 215123, PR China

<sup>c</sup> Key Laboratory of Plant Resources Conservation and Sustainable Utilization, Guangdong Provincial Key Laboratory of Applied Botany, South China Botanical Garden, Chinese Academy of Sciences, Guangzhou, Guangdong 510650, PR China

<sup>d</sup> Guangzhou Welbon Biological Technology Co., Ltd, Guangzhou, Guangdong 510663, PR China

## ARTICLE INFO

### Article history:

Received 10 November 2016

Received in revised form 25 February 2017

Accepted 27 February 2017

Available online 28 February 2017

### Keywords:

Eggless cake

Soybean protein isolate

Emulsifier

Batter

Fourier transform infrared spectroscopy

(FTIR)

Atomic force microscopy (AFM)

Ingredient substitution

Starch

## ABSTRACT

To evaluate the feasibility of substituting eggs in yellow cake by a mixture of soybean proteins, plant polysaccharides, and emulsifiers, the batter properties, including specific gravity and viscosity; cake properties, including specific volume, texture, colour, moisture, microstructures, and structural properties of starch and glutes of the replaced cake and traditional cake containing egg, were evaluated. Replacing eggs with a soy protein isolate and 1% mono-, di-glycerides yielded a similar specific volume, specific gravity, firmness and moisture content (1.92 vs. 2.08 cm<sup>3</sup>/g, 0.95 vs. 1.03, 319.8 vs. 376.1 g, and 28.03% vs. 29.01%, respectively) compared with the traditional cakes baked with eggs. Structurally, this formulation comprised dominant gliadin aggregates in the size range of 100–200 nm and glutenin networking structures containing fewer but larger porosities. The results suggest that a mixture of soybean proteins and emulsifier is a promising substitute for eggs in cakes.

© 2017 Elsevier Ltd. All rights reserved.

## 1. Introduction

Cakes are one category food globally consumed and favoured by people, with a steadily growing global market (Wilderjans, Luyts, Brijs, & Delcour, 2013). Cakes are served in different shapes, sizes, and categories, but are made using a few basic ingredients, including eggs. It is important to incorporate air during batter mixing to form and maintain the foam of the batter. Egg white proteins are responsible for the good foaming capacity, emulsification, stabilisation, elasticity, and other properties (Wilderjans et al., 2013). Eggs are also used as binding, colouring, and flavouring agents in yellow cakes (Kiosseoglou, 2003).

However, traditional cakes made with eggs are not suitable for consumers with special dietary restrictions; e.g. for religious reasons, health concerns, or personal lifestyle choices. Eggs contain high amounts of cholesterol, a high dietary intake of which has been linked to cardiovascular diseases. Although the cholesterol

limit has been removed from the 2015–2020 Dietary Guidelines for Americans, dietary limitations of cholesterol are still recommended to elderly people or people with previous incidents of heart disease. An additional concern is that some people are allergic to egg components. Moreover, eggs make up about 50% of the ingredient cost in cakes (Arozarena, Bertholo, Empis, Bunger, & Sousa, 2001); therefore, the baking industry is very interested in developing egg substitutes to partially or completely replace eggs to produce cakes.

Previous researchers investigated the possibility of various ingredients as egg substitutes in cakes. In cereal products, glutes, namely gliadin and glutenin, are vital for their unique traits of viscoelasticity (Wilderjans, Pareyt, Goesaert, Brijs, & Delcour, 2008). Different types of proteins have been tested as substitutes for eggs in cakes (Arozarena et al., 2001; Jyotsna, Sai Manohar, Indrani, & Venkateswara Rao, 2007; Rahmati & Mazaheri Tehrani, 2014). However, their success has been limited, suggesting that the substitute proteins have different functions compared with eggs and additional components are needed to make equivalent quality cakes using eggless recipes. Apart from proteins used to replace eggs in cakes, polysaccharide hydrocolloids or emulsifiers as egg

\* Corresponding author at: Food Science and Technology Programme, c/o Department of Chemistry, National University of Singapore, 3 Science Drive 3, Singapore 117543, Republic of Singapore.

E-mail address: [chmyngs@nus.edu.sg](mailto:chmyngs@nus.edu.sg) (H. Yang).

substitutes have also been evaluated. Polysaccharides were applied as baking additives to further enhance the shelf-life or physical properties (Gómez, Ronda, Caballero, Blanco, & Rosell, 2007; Ratnayake, Geera, & Rybak, 2012), while emulsifiers were to stabilise the foams (Sahi & Alava, 2003) or enhance the flavour (Mao, Roos, Biliaderis, & Miao, 2015).

Currently, the majority of research on the modification of cake formulations has focused on the physicochemical properties of the batter and cakes. Changes in the physical attributes are likely derived from the changes of the molecular structures. Thus, many studies have used Fourier transform infrared (FTIR) to analyse the structural alterations upon treatments (Dong, Zhang, Tang, & Wang, 2015; Sow & Yang, 2015; Wang et al., 2014). Compared with FTIR spectroscopy, atomic force microscopy (AFM) is a newer addition to food structural analysis. Lacking vacuum conditions and complicated sample pre-treatment, AFM is regarded as a convenient and non-destructive analytical approach (Liu, Tan, Yang, & Wang, 2017; Liu & Wang, 2011). Thus, it has been applied widely to investigate the morphologies of many macromolecules, including fruit polysaccharides (Chong, Lai, & Yang, 2015), starches (An et al., 2011; Du, An, Liu, Yang, & Wei, 2014) and fish gelatin (Feng, Fu, & Yang, 2017; Feng, Ng, Mikš-Krajnik, & Yang, 2017; Sow & Yang, 2015).

The aim of this project was to develop egg substitutes for cakes using plant based proteins and polysaccharides. For this purpose, we used soybean protein isolate (SPI) together with plant polysaccharides and emulsifiers. The functionality of these ingredients was evaluated and compared with egg proteins by measuring the batter and cake properties, as well as the structural properties of starches and glutens.

## 2. Materials and methods

### 2.1. Materials

A standard yellow cake recipe from Ratnayake et al. (2012) was used, with slight modifications. The traditional formulation comprised wheat flour (27.88%), baking powder (0.84%), milk (16.73%), sugar (32.26%), canola oil (8.36%), and eggs (13.93%). In the eggless recipes, eggs were replaced by SPI (3.30%) and other additives.

Wheat flour was provided by Prima Ltd., Singapore. Other ingredients, including fresh eggs (Seng Choon Farm Pte Ltd., Singapore), baking powder (Bake King® from Gim Hin Lee Pte Ltd., Singapore), pasteurised skimmed milk (Emborg™ from Uhrenholt Co., Middelfart, Denmark), sugar and canola oil were obtained from a local supermarket (Fairprice, Singapore). SPI (SUPRO 120®; 90% d.b.), xanthan gum (XN) (Grindstead®) and soy lecithin (SL) (SOLEC®) were obtained from Danisco (S) Pte Ltd. (Singapore). Mono and diglycerides (MDG) (Emulpals 110®) was obtained from Palsgaard Asia Pacific Pte Ltd. (Singapore) and modified cornstarch was obtained from Ingredient Singapore Pte Ltd. (Singapore). Sodium hydroxide, hexane, and ethanol were obtained from VWR Singapore Pte Ltd. (Singapore, Singapore). Dithiothreitol and *n*-propanol were provided by Bio-Rad Laboratories, Inc. (Hercules, CA, USA) and TCI Co. Ltd. (Tokyo, Japan), respectively. All the ingredients were of food grade and the chemical reagents were of analytical grade.

### 2.2. Cake batter property determination

The eggs were homogenised to mix the albumen and yolk at speed 1 using a professional KitchenAid mixer (St Joseph, MI, USA). The ingredients were then mixed together for 1 min at speed 1 (60 rpm) using the balloon whisk attachment and subsequently

mixed at speed 6 (180 rpm) for 4 min. The specific gravity of the batter was measured by filling a cylindrical cup with batter. The specific gravity was calculated as the ratio of mass of the batter to the mass of water used at 25 °C using the same cup. Batter viscosity was measured using a rapid viscosity analyser series 4 (Newport Scientific Pty Ltd., Jessup, MD, USA) (Wilderjans et al., 2008). The programme used to set the parameters of the analysis was thermocline for windows version 2.4 (Newport Scientific Pty Co., Ltd.). Cake batter (25g) was used and the temperature profile was set according to the internal temperature of the batter during baking.

### 2.3. Cake baking and characterisation of the final products

The cake batter (250 g) was placed in a cylindrical baking tin (height = 70 mm and bottom diameter = 100 mm) and was baked in a convection oven (Fabricant Eurfours®, Gommegnies, France) at 180 °C for 35 min. After baking, the cakes were taken out and cooled at room temperature for 60 min before further analysis.

#### 2.3.1. Volume and moisture content of cakes

The volume of the finished product was measured using a stable microsystem volscan profiler 600 (Stable Micro Systems Ltd., Surrey, UK). Triplicate determinations were performed for each formulation. The specific volume of the cake (cm<sup>3</sup>/g) was determined by measuring the cake volume (cm<sup>3</sup>) divided by the mass (g). The moisture content of the samples was measured according to the AOAC (1980) procedure. A cake crumb (about 2.0 ± 0.1 g) placed in a metal dish, weighed, and placed in an oven (100 °C) for at least 24 h. Upon removal from the oven, the dish was cooled to room temperature in a desiccator before the crumb was re-weighed. The moisture content was calculated by the weight loss divided by the original sample weight.

#### 2.3.2. Colour and texture measurement

The colour of the cake crumb was measured using a Kinoca Minolta CM-5 spectrophotometer (Konica Minolta Holdings Inc., Tokyo, Japan). Plastic cling wrap was used as a reference. The results reported represented six measurements for each formulation. The overall colour difference was calculated as

$$\Delta E = \sqrt{(L^* - L_{ref}^*)^2 + (a^* - a_{ref}^*)^2 + (b^* - b_{ref}^*)^2}$$

The textural properties of the cakes were measured using a TA-XT2i texture analyser (Stable Micro System Ltd., Surrey, UK) according to the methods of Ratnayake et al. (2012), with slight modifications. Cake samples were cut into cubes (20 mm × 20 mm × 20 mm). A double compression test was performed using a 25 mm cylinder probe. Triplicates determinations were performed for each formulation. In the compression test, the parameters were set as: pre-test speed = 5 mm/s, test speed = 1 mm/s, post-test speed = 1 mm/s, and the compression distance = 10 mm.

### 2.4. Sensory evaluation

Sensory analyses were carried out in an air-conditioned (22 °C) sensory room with the lighting adjusted so that the colours of the samples could be evaluated. Water was provided for palate cleansing. Cake samples were cut into cubes of dimension 2 × 2 × 2 cm<sup>3</sup> and placed in sensory cups with a cover to prevent drying. Each cup was randomly coded with a three-digit number. Quantitative descriptive analysis (QDA) was applied for the sensory profiling of the cake samples, according to the method proposed by Stone and Sidel (2004).

The panellists (3 males and 8 females, ages 20–24) evaluated the products in a sensory evaluation room. A standardised vocabulary to describe the different attributes of the cakes was generated based on the results of the panellists in the pre-sensory evaluation. Overall, 10 sensory attributes covering appearance, aroma, taste, and texture were generated. The panellists were given reference standards to further reinforce their perception of an attribute of the cake sample. Sensory panellists were required to rate six coded eggless cake samples and one coded control (cake baked with eggs), based on the specific attributes using a continuous 9-point hedonic scale in which 1 as the “weakest” and 9 was the “strongest”. Finally, the panellists were asked to go through all the cake samples again and evaluate them using the previously determined references for all attributes, including appearance, aroma, taste, and texture.

### 2.5. Wide angle powder XRD determination

The X-ray diffraction (XRD) diffractogram of the freeze-dried crumb samples were collected with a Siemens D5005 diffractometer (Bruker AXS, Karlsruhe, Germany), equipped with a copper tube operating at 40 kV and 40 mA. The recording  $2\theta$  range was 7–30° with a step size of 0.01° and measurement time of 1 s per  $2\theta$  interval (Primo-Martín, van Nieuwenhuijzen, Hamer, & van Vliet, 2007). After the baseline was subtracted and the  $K\alpha_2$  peak was stripped, the integrated areas were measured using DIFFRAC plus EVA 10.0.1.0 (Bruker AXS, Karlsruhe, Germany). The relative crystallinity was calculated using the following equation (Miao, Jiang, Zhang, Jin, & Mu, 2011):

$$X_c = A_c / (A_c + A_a),$$

where,  $X_c$  is the relative crystallinity, and  $A_c$  and  $A_a$  are the integrated areas of the crystalline and amorphous regions, respectively.

### 2.6. FTIR analysis

#### 2.6.1. Extraction of starches and glutes

Cake samples were freeze-dried, ground in a mill, and defatted with hexane three times, according to Wilderjans et al. (2008). The defatted sample (2 g) was soaked in 10 mL of 70% ethanol at 80 °C in a water bath for 18 h. After the steep liquor was drained, 5 mL of distilled water was added to grind the sample. The residue after filtration through a 100-mesh sieve was washed with 20 mL of water and then the wash-throughs were re-sieved. The obtained wash-throughs were screened using a 200-mesh sieve followed by centrifugation at  $3000 \times g$ . Subsequently, 10 mL of 0.5 M NaOH solution was added with stirring for 20 min, followed by centrifugation. The pellet was extracted with 10 mL of H<sub>2</sub>O/toluene (4:1) mixture. The supernatant was collected and centrifuged to obtain the starch isolate (Xie, Cui, Li, & Tsao, 2008).

The gluten fractions were separated based on the Osborne approach (Lookhart & Bean, 1995). The defatted samples (2 g) were mixed with 10 mL of deionised water and then 10 mL of 0.5 M NaCl aqueous solution for 30 min to remove sugar, starch, albumin, and globulin. After the suspensions were centrifuged at  $7000 g$  for 5 min, the pellet was rinsed with deionised water before being treated with 10 mL of 70% ethanol for 30 min at 4 °C twice. The supernatants obtained after centrifugation were the gliadin fraction. The residue was added with 5 mL of dithiothreitol (1%) and *n*-propanol (50%) mixture solution at 4 °C, extracted for 30 min, and centrifuged to obtain the glutenin subunits.

#### 2.6.2. FTIR spectra interpretation

The isolated dry starch or gluten subunits samples (about 2 mg) were mixed with 200 mg of KBr (Merck KGaA, Darmstadt, Germany) and made into pellets. The spectrum was collected using a Spec-

trum One FTIR spectrometer (PerkinElmer, Waltham, MA, USA) at 4 cm<sup>-1</sup> resolution for 32 scans in the range of 4000–450 cm<sup>-1</sup>.

The spectra of the starch samples were analysed with Omnic software 8.2 (Thermo Fisher Scientific Inc., Waltham, MA, USA). After baseline correction and normalisation, the peak positions were recorded and assigned. Fourier self-deconvolution was also applied to the range of 1100–950 cm<sup>-1</sup> in each spectrum, with a bandwidth of 30 cm<sup>-1</sup> and an enhancement factor of 1.5, according to Liu's study (2014). The ratio of the absorbance intensities at 1047 and 1022 cm<sup>-1</sup> was then obtained from the deconvoluted spectra.

After assigning the amide bands on the spectra of gliadin and glutenins, the amide I band at the range of 1700–1600 cm<sup>-1</sup> was further studied by deconvolution for glutenins. The bandwidth was set at 30 cm<sup>-1</sup> and the enhancement factor was 1.3. The deconvoluted spectra were subsequently fitted using the Gaussian peak fit function in the OriginPro 9.0 software (OriginLab, Northampton, MA, USA), based on the research of Byler and Susi (1986). The relative percentages of the secondary structure components were acquired from the relative integrated areas of the corresponding fitted peaks. In addition, the amide III band at 1350–1200 cm<sup>-1</sup> was analysed using the derivative spectra yielded from the eleven-point, two-degree polynomial function; the spectra were then multiplied by -1 to invert the peaks. Finally, the OriginPro 9.0 software was used to locate the peaks and calculate the integrated areas.

### 2.7. AFM analyses of glutes

The diluted solution (10 µL in 0.1 mg/mL) of glutes was dropped onto a freshly exfoliated mica sheet and dispersed with a blower. After drying at room temperature, the structural characterisation of the protein fraction was analysed using a table top AFM (TT-AFM) (AFM workshop, Signal Hill, CA, USA), according to the method of Sow and Yang (2015). The AFM was equipped with an AppNano ACLA-10 probe (Applied NanoStructures, Mountain View, CA, USA) with resonance frequencies at 145–230 kHz and force constants of 36–90 N/m. The qualitative and quantitative analyses of the images were carried out using the AFM offline software, Gwyddion (<http://gwyddion.net>), based on at least 20 images for each sample. For gliadin, the diameters of the spherical aggregates were measured and categorised into several range groups. The relative percentages of each size range were calculated. For the images of glutenin, the thickness of the thin layers and the networking structures (pore size distribution, pore number, and pore area in 25 µm<sup>2</sup>) were recorded for each group.

### 2.8. Statistical analysis

Results were expressed as the mean ± standard deviation. Differences among different groups were analysed using analysis of variance (ANOVA) and Duncan's multiple range test via the SAS 9.4 software (SAS Institute Inc., Cary, NC, USA). Comparisons among groups that yielded a *P* value < 0.05 were considered significant.

## 3. Results and discussion

### 3.1. Physical properties of eggless cakes

#### 3.1.1. Batter properties of eggless cakes

Previous reports indicated that the batter properties affect the volume of the finished cakes (Ashwini, Jyotsna, & Indrani, 2009; Gómez et al., 2007). Thus, the effect of egg substitution on the batter properties was studied to determine its effect on the specific

volume of the cake (Table 1). The substitution of eggs by SPI led to a significant increase in the batter specific gravity (1.03 vs. 1.13) and a decrease in the specific volume with respect to the control (2.08 vs. 1.47 cm<sup>3</sup>/g). Addition of 1% of any emulsifier, or in combination with XN, increased the specific volumes of the SPI cakes to a level similar to that of the control cake. The baked cake volume is a result of the stabilising proteins that form a strong thermal gel that ensures cake structure; high volume indicates the presence of proteins with good gel forming properties, such as eggs (Kiosseoglou, 2003). The limitations of SPI in terms of foam stability and gelling properties were responsible for the poor specific volume in eggless cakes (Xie & Hettiarachchy, 1998) (Table 1). Therefore, the results suggest that substitution with SPI can't guarantee the specific gravity of the batter and the specific volume of the cakes. However, the presence of baking additives, such as XN, MDG, and SL, reduced the specific gravity of the batter significantly ( $P < 0.05$ ) compared with the eggless cake batters (SPI only).

The viscosity of the eggless cake batters containing SPI (23.45 Pa·s) was significantly higher than the control batter (9.42 Pa·s). XN further increased the viscosity, whilst the emulsifiers decreased it. However, combinations of XN and emulsifiers (MDG or SL) reduced the viscosity and improved the volume of the cake produced. The higher viscosity of the eggless cake batter was caused by the high water binding capacity of SPI and the ability of XN to bind water molecules was responsible for the further enhancement (Gómez et al., 2007). In terms of the reduction effect using the combination of XN and emulsifiers, this was probably caused by the delay of starch gelatinisation resulting from the presence of the emulsifiers. The delay allowed for more expansion of the cake batter and a higher cake volume (Majzoobi, Ghiasi, Habibi, Hedayati, & Farahnaky, 2014). In summary, although the viscosity of the eggless batter was significantly higher than the control cake, the eggless cakes containing emulsifiers (R3–R6) showed comparable specific gravities and specific volumes compared with the control cakes.

### 3.1.2. Crumb properties of eggless cakes

In addition to the batter properties, the quality of the final cake products, crumb textures, colours, and moisture contents, are of great importance to evaluate the eggless cakes. The effects of different ingredients on the textural properties of eggless cakes using SPI as a protein substitute for egg are also shown in Table 1. In general, the replacement of eggs by SPI increased the firmness of the eggless cake but decreased its springiness. An increment in firmness of sponge cake was also observed in the study of Majzoobi et al. (2014). Starch gel influences crumb firmness; therefore, it was postulated that the high water binding activity of SPI reduced the free water, decreased the amylose content, and thus reduced cake softness (Wilderjans et al., 2008). The protein aggregation in cake crumb is associated with the springiness; therefore, the differ-

ent protein subunits in SPI (glycinin and  $\beta$ -conglycinin) were hypothesised to be responsible for the differences in springiness of eggless cakes (Wilderjans et al., 2008). In addition, other components in egg yolk were demonstrated to aid the thermal stabilisation of the yolk gel (Kiosseoglou, 2003), further affecting the difference in the springiness of the control and eggless cakes. Selected macroscale images of crumb morphology of cakes made from egg substitution using soy protein isolate (SPI) and baking additives are shown in Fig. S1. Since the sensory evaluation also includes the morphology and appearance, the macroscale morphology images could be applied for analysing the reasons links to the sensory evaluation results.

The addition of 0.1% XN, 1% emulsifier, and a combination of both to the SPI-based eggless cake reduced the springiness of the eggless cakes significantly (Table 1), indicating that the addition of XN altered the gelation properties of the proteins. Based on the differences in the emulsification mechanisms of proteins and emulsifiers, it was possible that the 1% MDG used in the current study was the dominant stabiliser, leading to a less springy eggless cake. The firmness of the eggless cakes was also reduced remarkably upon addition of 1% MDG, probably by improving the aeration capability of the cake batters. In terms of the combination of XN and any emulsifier, the firmness was not significantly different to that of the cakes containing only the protein and emulsifier (Table 1). It was hypothesised that the addition of emulsifiers was responsible for the reduction in the crumb firmness of the eggless cakes (Ashwini et al., 2009).

Table S2 shows the  $L^*$ ,  $a^*$  and  $b^*$  values (light and colour measures) of the control cake and the eggless cakes containing SPI. Eggless cakes using SPI were darker than the control (the crumb  $L^*$ -value of the control cake vs. the eggless cake: 77.88 vs. 75.36). In addition, eggless cakes containing SPI had a significantly higher  $a^*$ -value but a lower  $b^*$ -value than the control cake. The colour of the cake crust is affected by the Maillard reaction and caramelisation during baking, whereas the crumb colour of the cakes is affected by the ingredient used and its formulation (Majzoobi et al., 2014). Overall, although the colour parameters of the eggless cakes were not very desirable, the firmness and moisture content of cakes with SPI and 1% of any emulsifier mimicked those of the traditional cakes successfully.

The sensory evaluation results of the eggless cakes against the control cake are presented in Table S3. For the parameters of beany taste, eggy taste, overall aroma, and stickiness or adhesiveness, the eggless cakes were perceived to be significantly different from the control. This also affected the overall consumer acceptance of the cakes, as can be seen by the fact that the consumer acceptance of the control was somewhat higher than that of the eggless cakes. However, among all the eggless cakes, those with SPI + 1% MDG (R3) was deemed to have no significant difference compared with the control for most attributes, including consumer acceptance.

**Table 1**  
Batter, crumb and starch ordering parameters of eggless cakes using soy protein isolate (SPI) and other baking ingredients as egg replacers.

Group	Specific gravity	Initial viscosity (Pa·s)	Specific volume (cm <sup>3</sup> /g)	Firmness (g)	Springiness (%)	Moisture (%)	$X_c$	In (1047/1022)
Control	1.03 ± 0.04 <sup>B</sup>	9.42 ± 0.99 <sup>F</sup>	2.08 ± 0.13 <sup>A</sup>	376.1 ± 45.7 <sup>B</sup>	98.0 ± 4.0 <sup>A</sup>	29.01 ± 0.36 <sup>A</sup>	0.21 ± 0.03 <sup>B</sup>	0.55 ± 0.01 <sup>D</sup>
R1	1.13 ± 0.02 <sup>A</sup>	23.45 ± 3.00 <sup>D</sup>	1.47 ± 0.02 <sup>C</sup>	1028.2 ± 161.8 <sup>A</sup>	84.0 ± 5.0 <sup>B</sup>	27.43 ± 0.42 <sup>CDE</sup>	0.25 ± 0.01 <sup>AB</sup>	0.71 ± 0.01 <sup>A</sup>
R2 <sup>*</sup>	1.07 ± 0.01 <sup>AB</sup>	40.70 ± 1.18 <sup>A</sup>	1.54 ± 0.01 <sup>C</sup>	994.7 ± 340.5 <sup>A</sup>	82.0 ± 4.0 <sup>CD</sup>	27.73 ± 0.21 <sup>BC</sup>	0.25 ± 0.02 <sup>AB</sup>	0.59 ± 0.01 <sup>C</sup>
R3 <sup>*</sup>	0.95 ± 0.11 <sup>C</sup>	24.03 ± 1.71 <sup>D</sup>	1.92 ± 0.03 <sup>B</sup>	319.8 ± 51.9 <sup>BC</sup>	77.0 ± 1.0 <sup>E</sup>	28.03 ± 0.09 <sup>B</sup>	0.28 ± 0.01 <sup>A</sup>	0.63 ± 0.01 <sup>B</sup>
R4 <sup>*</sup>	0.95 ± 0.11 <sup>C</sup>	20.03 ± 2.16 <sup>E</sup>	1.86 ± 0.03 <sup>B</sup>	338.9 ± 100.5 <sup>BC</sup>	78.0 ± 1.0 <sup>E</sup>	27.07 ± 0.15 <sup>E</sup>	0.26 ± 0.01 <sup>A</sup>	0.59 ± 0.01 <sup>C</sup>
R5 <sup>*</sup>	0.96 ± 0.01 <sup>C</sup>	37.62 ± 2.74 <sup>B</sup>	2.15 ± 0.06 <sup>A</sup>	268.6 ± 27.4 <sup>C</sup>	82.0 ± 2.6 <sup>DE</sup>	27.27 ± 0.28 <sup>DE</sup>	0.26 ± 0.01 <sup>A</sup>	0.58 ± 0.01 <sup>C</sup>
R6 <sup>*</sup>	1.02 ± 0.02 <sup>C</sup>	32.50 ± 2.59 <sup>C</sup>	1.90 ± 0.06 <sup>B</sup>	252.3 ± 43.3 <sup>C</sup>	78.0 ± 3.0 <sup>E</sup>	27.50 ± 0.39 <sup>CD</sup>	0.25 ± 0.02 <sup>A</sup>	0.61 ± 0.04 <sup>BC</sup>

$X_c$ : Relative crystallinity obtained from X-ray diffraction (XRD); In (1047/1022): Intensity ratio of peaks at 1047 and 1022 cm<sup>-1</sup> in Fourier transform infrared (FTIR) spectra.  
R1: SPI; R2: SPI + 0.1%XN; R3: SPI + 1% MDG; R4: SPI + 1% SL; R5: SPI + 0.1%XN + 1% MDG; R6: SPI + 0.1%XN + 1% SL. SPI – soy protein isolate; XN – xanthan gum; MDG – mono, diglycerides; SL – soy lecithin. Values in the same column with different letter indicate significant difference by the Duncan's multiple range test ( $P < 0.05$ ).



### 3.2. Structural properties of starches

To better understand the mechanisms of physical property changes, the conformations of starch and glutens were studied. The freeze-dried cake samples were subject to XRD analysis to measure the ordering of the molecules, mainly starches. Among all the diffractograms (Fig. S2), only the broad peak at a  $2\theta$  angle of about  $20^\circ$  referred to the crystalline V-type amylose-lipid complexes (Primo-Martín et al., 2007). The relative crystallinities of the eggless cakes were slightly higher than those of the conventional cakes, implying that the substitution of egg components slightly decreased the amorphous region between the double helices of starches.

To understanding the conformational differences of starch in the different cakes, FTIR analysis was conducted, and the spectra are displayed in Fig. 1a. No obvious shifts in peak positions were observed, implying that the substitution of eggs had little impact on the basic skeletal structures of starches. The bands at around  $3434\text{ cm}^{-1}$ , associated with vibrations of various hydroxyl groups (Ji et al., 2015), were much stronger in the cakes containing SL or combinations of XN and emulsifiers (R4–R6). This might indicate that the inclusion of SL and XN increased the amount of inter- and intra-molecular hydroxyl groups in starches. The relative intensities at  $1021$ ,  $1083$ , and  $1156\text{ cm}^{-1}$  (C–O stretching) indicate the relative content of inter-chain hydrogen bonding in starches (Ji et al., 2015). The peaks at  $1083\text{ cm}^{-1}$  in the control group were slightly stronger than those of the eggless groups, which might suggest an interfering effect on the hydrogen bonds between starch chains when SPI was present. For the eggless cakes, the

decreasing trend of intensities starting from  $1083\text{ cm}^{-1}$  suggested a reinforcing effect of the additives.

A new peak at about  $1743\text{ cm}^{-1}$ , assigned to the carbonyl stretching vibration in esters, was detected in the spectra of starches in cakes containing SPI, SPI + 0.1% XN, SPI + 1% MDG, and SPI + 0.1% XN + 1% MDG. The presence of the  $1743\text{ cm}^{-1}$  peak suggested the formation of new cross-linking with ester bonds (Liu et al., 2014). The recipe with SPI and 0.1% XN possessed the highest amount of this type of crosslinking because of the synergic effects, followed by SPI only, and the combination of SPI and MDG (R3, R5). Nevertheless, the cakes with SL did not show peaks at  $1743\text{ cm}^{-1}$ , which was attributed to the existence of lecithin. A similar phenomenon might also happen in the batter matrix of the control cake, in which the phosphate and choline groups occupied the binding site for crosslinking, thus disturbing the network formation.

Absorption peaks at about  $1047$  and  $1022\text{ cm}^{-1}$  were characteristic of the vibrations of C–O–H bending at crystalline and amorphous regions. However, the intensity ratio of the peaks at  $1047$  and  $1022\text{ cm}^{-1}$ , which can reflect the relative crystallinity, conflicted with the XRD results. This was probably caused by the differences in determination principles and scopes between the two analytical methods. FTIR is more sensitive to short-scale ordering in the double helices, while only a longer range of crystallinity; i.e., the ordered packing of double helices, can be accepted as a real crystalline region in XRD (Miao et al., 2011; Primo-Martín et al., 2007). Although the current results showed that eggless cakes containing SL were much similar to the control cake, the physical properties of the final SL cakes did not have significant advantages

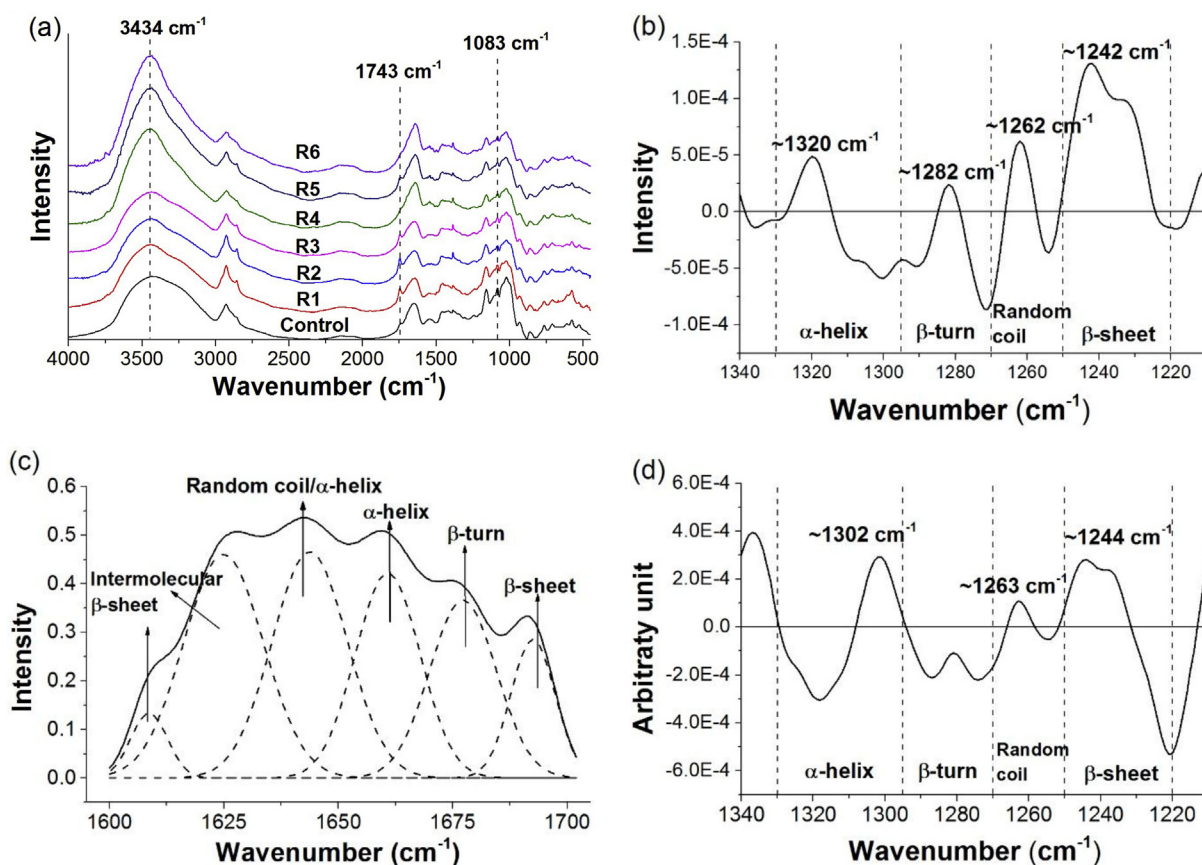


**Fig. 1.** (a) Fourier transform infrared (FTIR) spectra of starches in cakes made using different recipes; (b) Inverted second derivative spectra of gliadin in the amide III region ( $1350\text{--}1200\text{ cm}^{-1}$ ); (c) Curve fitting in deconvoluted FTIR spectra of glutenin in amide I (Solid line: deconvoluted curve; dashed lines: fitted peaks); (d) Inverted second derivative spectra of glutenin in amide III region. R1: SPI; R2: SPI + 0.1% XN; R3: SPI + 1% MDG; R4: SPI + 1% SL; R5: SPI + 0.1% XN + 1% MDG; R6: SPI + 0.1% XN + 1% SL. SPI – soy protein isolate; XN – xanthan gum; MDG – mono, diglycerides; SL – soy lecithin.

over the other eggless cakes, suggesting that the structure of starch was not a dominant feature affecting the final cake quality.

### 3.3. Structural properties of glutens

#### 3.3.1. FTIR analysis of glutens

The structural properties of the other major components, gliadin and glutenin, were also investigated. Considering the drawback that the amide I bands are interfered with easily when the water vibration absorbance and the composition peaks overlap heavily (Seabourn, Chung, Seib, & Mathewson, 2008), the amide III regions were also analysed to provide complementary information. The results revealed that the spectra needed further resolution improvement after Fourier self-deconvolution; therefore, the second derivatives were conducted directly in this region (Seabourn et al., 2008; Wang et al., 2015). The structural changes arising from the substitutions were studied by assessing the secondary structures of gliadin in the second derivative FTIR spectra.

As shown in Table 2,  $\beta$ -sheet structures were dominant among the secondary structures in all control and eggless groups. The  $\beta$ -sheet contents increased after the addition of SPI and any one of the additives (R1–R3), except for the combination of SPI and SL, suggesting an increase in the intermolecular interactions in gliadins. The combination of SPI, XN, and MDG had comparable impacts on gliadin secondary structures as SPI and SL. Interestingly, adding XN into the cakes with SPI and SL reduced the  $\beta$ -sheets significantly and converted them to random coils and helical structures. This might be attributed to the slightly charged property of SL, as it binds to proteins via hydrophobic interactions and the remaining phosphate groups repel each other to loosen the molecules, leading to weakened intermolecular interactions arising from  $\beta$ -sheets and looser molecules being converted into coils. Gliadin is rich in proline; therefore, the  $\beta$ -turn conformation could be more favoured. Overall, the gliadins in SPI groups all differed from the control cake, although the cakes with R4 and R5 were similar to the control cake with respect to their secondary structures.

The behaviour of the “loop and train” (Belton, 1999) conformation in glutenins is essential to the structural and physicochemical properties of glutens. The influence of the egg substitutes can arise from alteration of the repetitive domains, probably by acting as

connectors for intermolecular  $\beta$ -sheets. As only the FTIR spectra in the amide I region can differentiate the sub-types of  $\beta$ -sheets (Sivam, Sun-Waterhouse, Perera, & Waterhouse, 2012; Wang et al., 2014), the analysis of the spectra was based on both amide I and amide II regions.

In Table 2, the intermolecular  $\beta$ -sheets contents of eggless cakes increased remarkably to more than 25.10% compared with that of the control group (21.72%). This suggested that the substitutes improved the connections among the domains at the “train” part. Interestingly, for the groups with SPI and one emulsifier, opposite effects on the intermolecular  $\beta$ -sheet content were observed. Compared with the SPI only group (32.93%), the addition of MDG led to reductions in intermolecular  $\beta$ -sheet (25.10%) and SL had little effect on the contents (34.38%), implying that the connection effect from SPI did not prevail over the hindrance from MDG, while SL can bind to SPI and enhance its effects. By contrast, when XN was also combined in the substitute formula (R5, R6), other  $\beta$ -sheets (instead of intermolecular  $\beta$ -sheets) were converted to random coils. In brief, the eggless cakes without 0.1% XN (R1, R3, and R4) resembled the traditional cake better in terms of the secondary structures of glutenin.

#### 3.3.2. Morphology analysis of glutens

Besides the relative secondary structure contents of the glutens, their conformations at the mesoscale were also assessed using AFM. The general nanostructures of the gliadin fraction in cakes with SPI substituents were extended sheets mixed with aggregates of various sizes. Fig. 2b shows the quantification results conducted by separating the particles into groups according to their diameters and comparing the relative frequencies. The major components of gliadin,  $\alpha$ - and  $\gamma$ -gliadin subunits, mainly formed globular architectures, whereas some molecules with extra cysteines can act as glutenin (Kontogiorgos, 2011). The presence of SPI in the six eggless groups enlarged the size ranges of gliadin aggregates and shifted the mean towards larger sizes. This effect was enhanced upon the addition of XN but retained by SL. In contrast, when the cakes contained MDG or XN + MDG, the shifts towards larger size were not as obvious as cakes containing XN, SL or XN + SL, but with a similar distribution to the control group.

Table 3 summarises the AFM results for the glutenins. There were two major structures: thin layers with embedded or free

**Table 2**  
Percentage of secondary structure of gliadin and glutenin in eggless cakes with SPI replacers.

Groups	Secondary structure (%)			
	$\alpha$ -helix	$\beta$ -sheet <sup>^</sup>	$\beta$ -turn	Random coil
<i>Gliadin</i>				
Control	12.35 ± 0.61 <sup>B</sup>	69.35 ± 4.69 <sup>C</sup> (–)	2.98 ± 0.53 <sup>D</sup>	15.31 ± 3.92 <sup>B</sup>
R1 <sup>*</sup>	11.90 ± 0.91 <sup>B</sup>	74.01 ± 3.95 <sup>B</sup> (–)	3.61 ± 1.66 <sup>D</sup>	10.48 ± 2.75 <sup>C</sup>
R2 <sup>*</sup>	8.33 ± 1.10 <sup>C</sup>	77.06 ± 2.06 <sup>B</sup> (–)	0.06 ± 0.11 <sup>E</sup>	14.59 ± 1.00 <sup>B</sup>
R3 <sup>*</sup>	12.27 ± 1.68 <sup>B</sup>	86.85 ± 1.57 <sup>A</sup> (–)	0.20 ± 0.01 <sup>E</sup>	0.68 ± 0.11 <sup>D</sup>
R4 <sup>*</sup>	12.28 ± 1.59 <sup>B</sup>	67.49 ± 2.20 <sup>C</sup> (–)	10.52 ± 1.23 <sup>B</sup>	9.70 ± 1.40 <sup>C</sup>
R5 <sup>*</sup>	16.52 ± 1.31 <sup>A</sup>	69.12 ± 1.88 <sup>C</sup> (–)	6.72 ± 0.54 <sup>C</sup>	7.68 ± 1.41 <sup>C</sup>
R6 <sup>*</sup>	9.20 ± 0.56 <sup>B</sup>	42.00 ± 3.20 <sup>D</sup> (–)	28.43 ± 2.18 <sup>A</sup>	20.30 ± 0.70 <sup>A</sup>
<i>Glutenin</i>				
Control	37.53 ± 0.99 <sup>A</sup>	57.32 ± 0.90 <sup>A</sup> (21.72 <sup>d</sup> )	–	5.15 ± 1.87 <sup>B</sup>
R1 <sup>*</sup>	36.51 ± 0.24 <sup>AB</sup>	56.56 ± 1.45 <sup>A</sup> (32.93 <sup>ab</sup> )	–	6.92 ± 1.66 <sup>B</sup>
R2 <sup>*</sup>	30.69 ± 0.65 <sup>B</sup>	59.24 ± 0.58 <sup>A</sup> (35.14 <sup>a</sup> )	3.90 ± 2.40 <sup>A</sup>	6.17 ± 2.21 <sup>B</sup>
R3 <sup>*</sup>	37.03 ± 0.62 <sup>AB</sup>	58.30 ± 1.78 <sup>A</sup> (25.10 <sup>cd</sup> )	–	4.67 ± 2.36 <sup>B</sup>
R4 <sup>*</sup>	34.71 ± 4.37 <sup>AB</sup>	58.78 ± 1.84 <sup>A</sup> (34.38 <sup>a</sup> )	–	6.51 ± 3.72 <sup>B</sup>
R5 <sup>*</sup>	32.29 ± 1.88 <sup>AB</sup>	47.39 ± 2.49 <sup>B</sup> (27.79 <sup>bc</sup> )	–	20.32 ± 4.37 <sup>A</sup>
R6 <sup>*</sup>	37.29 ± 5.95 <sup>A</sup>	45.41 ± 7.41 <sup>B</sup> (29.55 <sup>abc</sup> )	–	17.30 ± 5.19 <sup>A</sup>

– Not detected.

<sup>^</sup> Values in the parentheses are the relative content of intermolecular  $\beta$ -sheet as compared with total secondary structures.

<sup>\*</sup> R1: SPI; R2: SPI + 0.1%XN; R3: SPI + 1% MDG; R4: SPI + 1% SL; R5: SPI + 0.1%XN + 1% MDG; R6: SPI + 0.1%XN + 1% SL. SPI – soy protein isolate; XN – xanthan gum; MDG – mono, diglycerides; SL – soy lecithin. Values in the same column with different letter indicate significant difference by the Duncan's multiple range test ( $P < 0.05$ ).

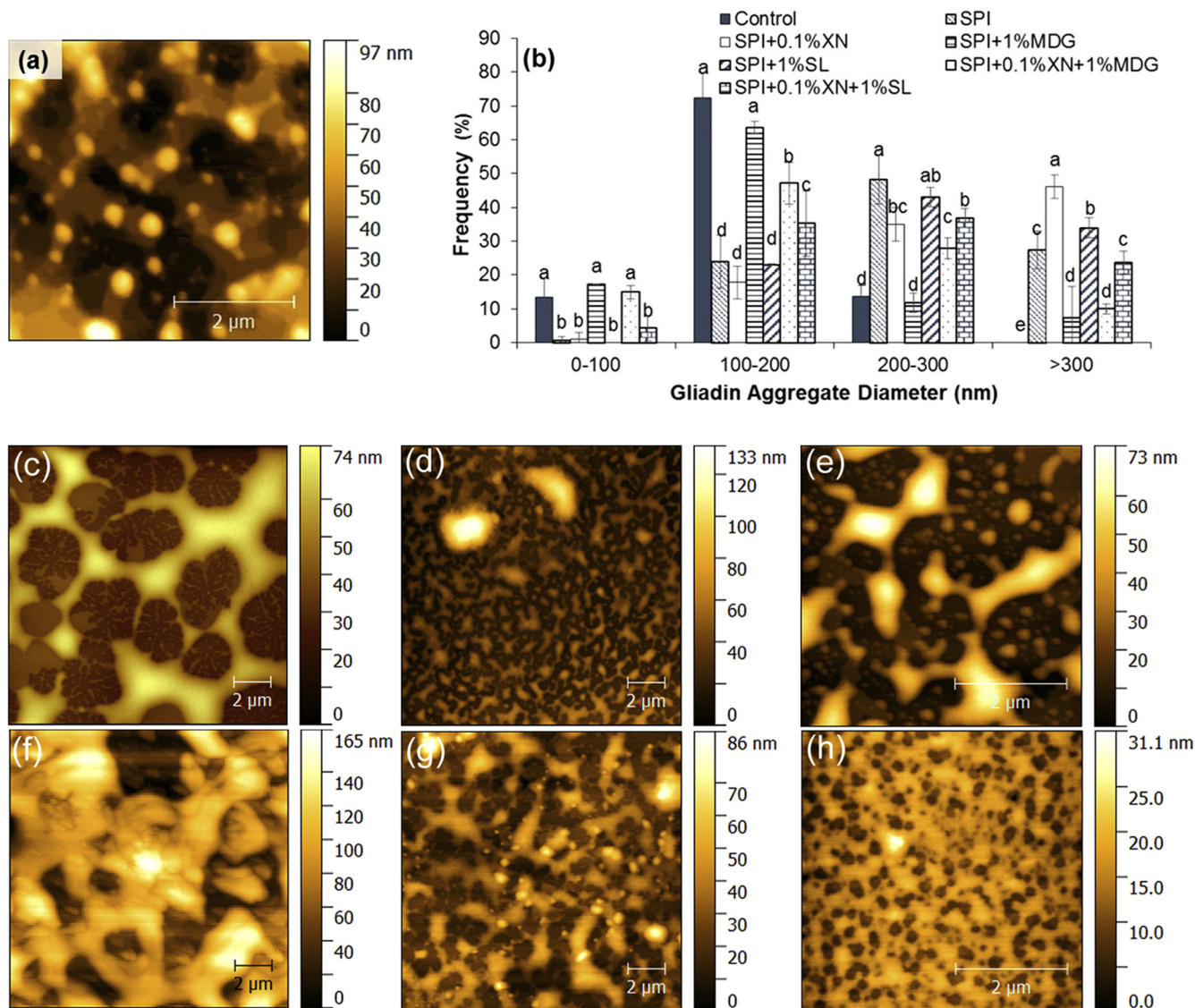


**Fig. 2.** Atomic force microscopy (AFM) results for gliadin and glutenin in cakes. (a) AFM image of gliadin aggregates; (b) Size distribution of gliadin aggregates; Porous structures of glutenin in (c) traditional cake and eggless cakes with (d) SPI + 0.1% XN, (e) SPI + 1% MDG, (f) SPI + 1% SL, (g) SPI + 0.1% XN + 1% MDG, (h) SPI + 0.1% XN + 1% SL. SPI – soy protein isolate; XN – xanthan gum; MDG – mono, diglycerides; SL – soy lecithin. Within each size range, groups with different letters are significantly different ( $P < 0.05$ ).

**Table 3**

Nanostructure of glutenin in eggless cakes with SPI replacers.

Group	Layer height (nm)	Pore number per 25 $\mu\text{m}^2$	Pore size distribution (nm) <sup>^</sup>			
			<100	100–500	500–1000	>1000
Control	6.90 $\pm$ 0.99 <sup>CD</sup>	4 $\pm$ 1 <sup>C</sup>	0%	2%	11%	87%
R1 <sup>†</sup>	7.40 $\pm$ 0.79 <sup>BC</sup>	–	–	–	–	–
R2 <sup>†</sup>	8.00 $\pm$ 0.80 <sup>B</sup>	25 $\pm$ 6 <sup>B</sup>	0%	77%	21%	2%
R3 <sup>†</sup>	7.08 $\pm$ 0.71 <sup>CD</sup>	9 $\pm$ 2 <sup>C</sup>	0%	4%	47%	49%
R4 <sup>†</sup>	7.23 $\pm$ 0.66 <sup>CD</sup>	7 $\pm$ 1 <sup>C</sup>	0%	0%	5%	95%
R5 <sup>†</sup>	6.61 $\pm$ 0.71 <sup>D</sup>	31 $\pm$ 4 <sup>B</sup>	0%	66%	20%	14%
R6 <sup>†</sup>	11.04 $\pm$ 1.8 <sup>A</sup>	93 $\pm$ 12 <sup>A</sup>	12%	88%	0%	0%

– Not detected.

<sup>^</sup> The pore size distribution was calculated based on 90 pores for the control group and at least 100 pores for the other groups.

<sup>†</sup> R1: SPI; R2: SPI + 0.1%XN; R3: SPI + 1% MDG; R4: SPI + 1% SL; R5: SPI + 0.1%XN + 1% MDG; R6: SPI + 0.1%XN + 1% SL. SPI – soy protein isolate; XN – xanthan gum; MDG – mono, diglycerides; SL – soy lecithin. Values in the same column with different letters indicate significant difference by the Duncan's multiple range test ( $P < 0.05$ ).

spherical aggregates, and porous structures. The thin sheets were possibly formed by the repetitive regions of aligned high molecular weight glutenin via hydrogen interactions and disulphide bonds

(Lagrain, Thewissen, Brijs, & Delcour, 2008). The heights of the layer were similar for all the groups at about 7 nm, except R2 and R6 (Table 3), which were slightly thicker (8.00 and 11.04 nm,



respectively). As the porosities were supposed to be in the hydrated region (Kontogiorgos, 2011), the absence of porosity in the SPI only cake (R1) may reflect a compacted conformation in glutenin. The compacted structure might be related to the high contents of intermolecular  $\beta$ -sheets, because they are associated with stronger interaction between the “loop” and the “train” regions.

Upon addition of the additives, the pore sizes decreased greatly, except the two groups with SPI and emulsifiers (R3 and R4) (Fig. 3e and f). However, the boundary of the pores in R3 was almost missing and the network was weakened. By contrast, R4 seemed to produce strong networking with thick walls. It should be pointed out that the porosity of R5 was small, but had different

layers above. The upper layers appeared to have a looser structure and resembled the porosity in the control group, which might have resulted from the combination effect of XN and MDG. To summarise, recipes R3, R4, and R5 could be potential candidates for substituting eggs in the traditional cakes with regard to the nanostructures of glutenin. However, when other parameters were taken into consideration, only the eggless cake with SPI + 1% MDG as replacement (R3) could fulfil most of the expectations.

#### 3.4. Cost analysis of eggless cake recipes

As is mentioned before, eggs account for a significant proportion of the cost of cakes; therefore, a cost analysis was conducted

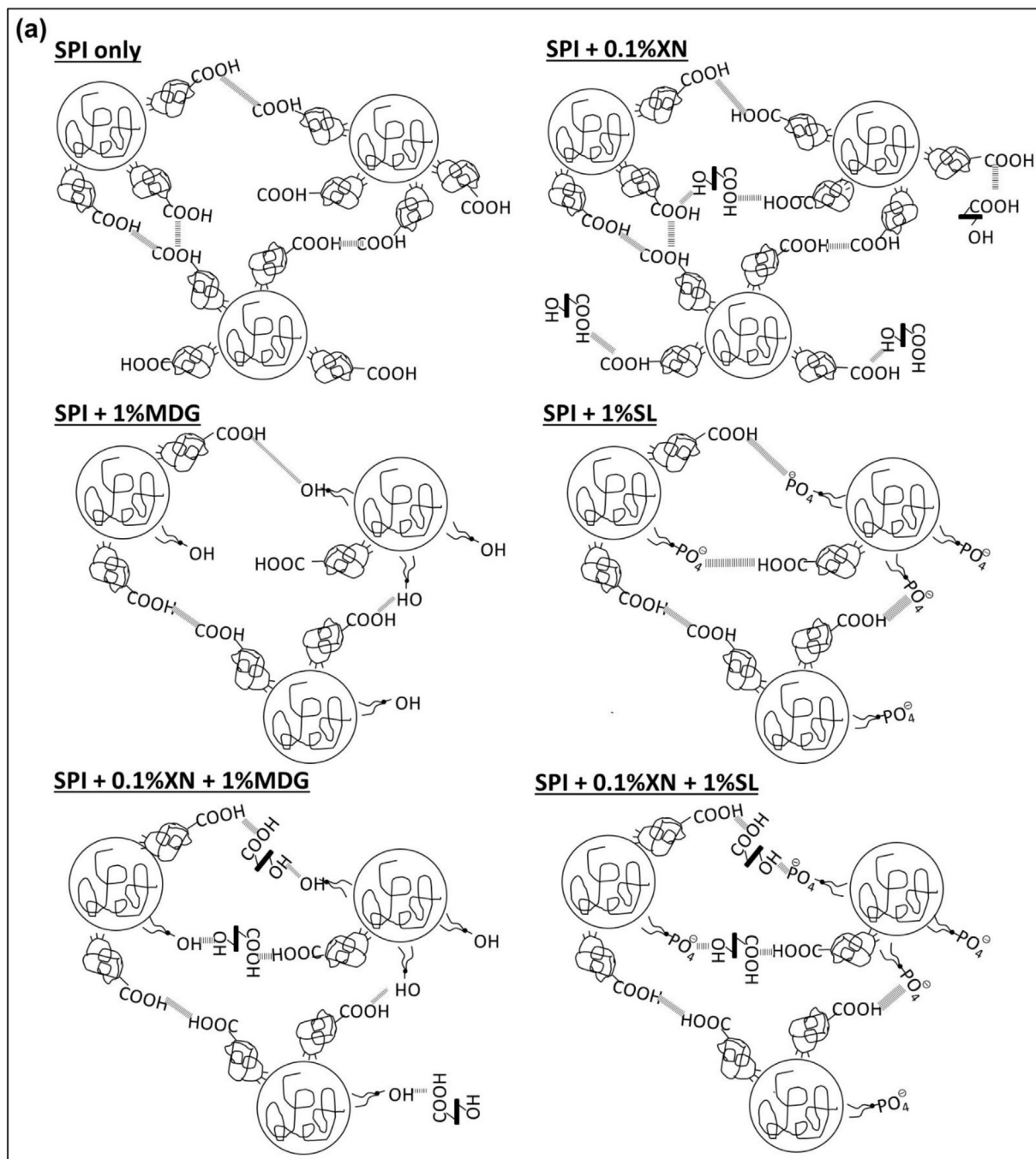


**Fig. 3.** Schematic diagram of (a) gliadin aggregation structures and (b) glutenin structures (side view) in cakes made using different recipes. SPI – soy protein isolate; XN – xanthan gum; MDG – mono, diglycerides; SL – soy lecithin.



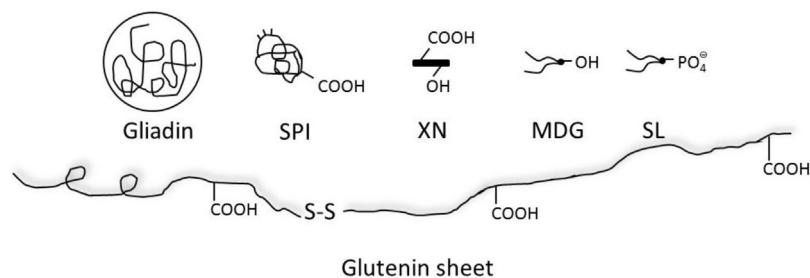
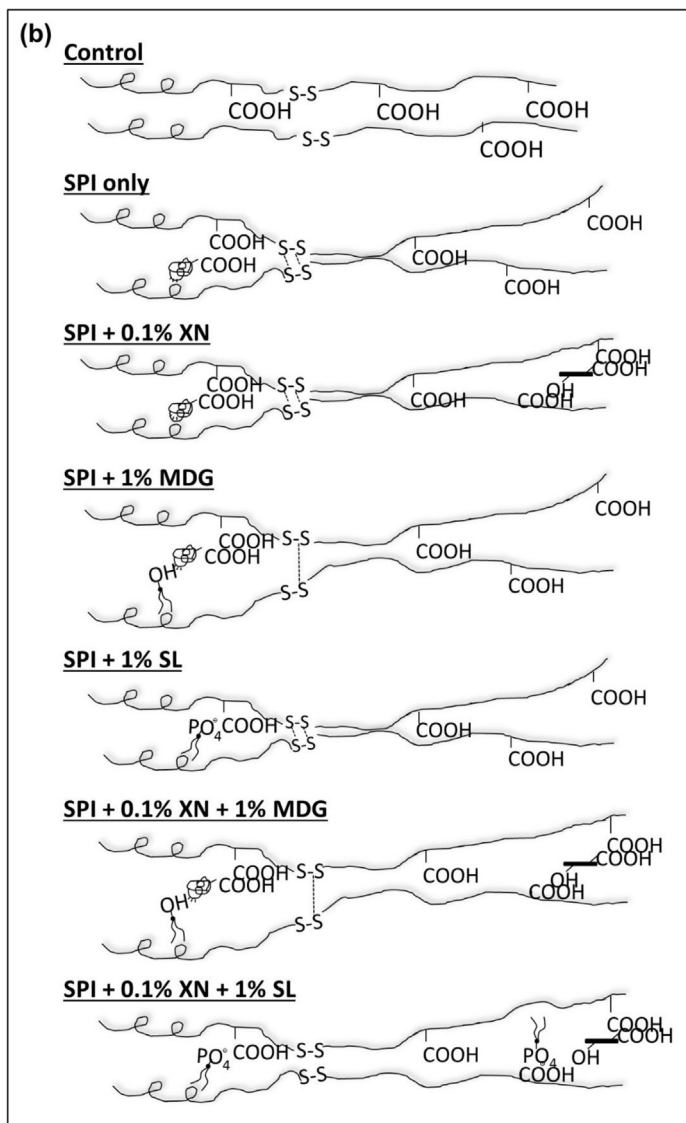


Fig. 3 (continued)

between the developed eggless cake recipe and traditional one. Table S4 indicated that upon substitution of eggs with SPI + 1% MDG, the batter cost was reduced by 13% compared with that of the traditional cakes (\$1.84/kg of batter for R3 vs. \$2.11/kg of batter for traditional).

### 3.5. Schematic modelling

Based on the structural analyses of gliadin and glutenin upon the addition of different egg substitutes, a schematic model was proposed for these two glutes. The possible mechanism of gliadin

is shown in Fig. 3a. Gliadin was rich in proline, leucine, and glutamine; therefore, the interaction at the outer surfaces with other molecules should be mainly hydrophobic interactions. SPI contains high levels of tryptophan, glutamic, and aspartic acid, leaving globular structures with some hydrophilic interacting positions with carboxylic groups.

SPI can work as an emulsifier and form a thin protein layer on the surface of small gliadin molecules via hydrophobic interactions. The “coated” spheres are then connected with others via hydrogen bonds, resulting in larger aggregates that were dominant in the range of 200–300 nm and >300 nm in the AFM results

(Fig. 2b). Further addition of XN strengthened hydrogen bonding, especially at the positions where the aggregates were distant. MDG and SL are fatty acid emulsifiers that can interfere with and replace some protein emulsifier molecules at the interface. As a result, some of the SPI bound on the gliadins were replaced by MDG or SL. MDG and SL both have polar heads that can take part in hydrogen bonding; therefore, the aggregation effects were not cancelled completely. In addition, SL is a much stronger hydrogen bond acceptor because of its charged phosphate group; therefore, some interactions can be compensated for and the degree of aggregation could be higher. Finally, the combination of XN in these two groups appeared to enhance the hydrogen bonding interactions slightly and the aggregate sizes were shifted to a higher range, according to the AFM analysis (Fig. 2b). Overall, among these substitutes, SPI + 1% MDG led to the weakest hydrophilic interaction and least aggregation, which resembled the structures of gliadin aggregates in the traditional cakes.

The schematic diagrams of the glutenin structures in different recipes are displayed in the side view of Fig. 3b. The glutenin sheets were separated and loosely piled in the flour, and some disulphide bonds, and hydrophilic and hydrophobic interactions were formed after mixing. When SPI was added, the parts that were originally separated because of low interaction could combine with SPI, increasing the intermolecular  $\beta$ -sheet content (21.72 vs. 32.93%) and layer heights (6.90 vs. 7.40 nm). XN connected the two positions with carboxylic groups over long distances. However, MDG and SL might compete with SPI for the hydrophobic binding sites and increase the hindrance between the glutenin sheets. Unlike MDG, SL is a stronger hydrogen bond acceptor than SPI; therefore, it can further link with glutenin and maintain the intermolecular  $\beta$ -sheet structures (25.10%). The existence of XN can only take effect at the positions with potential hydrogen bonding, but had little impact on the parts with more hydrophobic interactions. Similar to the gliadin aggregates, the favourable interactions between glutenins were promoted in the presence of SPI and 1% MDG. In the future, interactions among gluten molecules, starch molecules, plant polysaccharides and emulsifier molecules should be investigated for elucidating the ingredient substituted cake system (Liu et al., 2017; Xin et al., 2010; Yang, Wu, Ng, & Wang, 2017).

#### 4. Conclusions

SPI with 1% MDG (R3) could be used as an egg substitute in cake formulations. This combination resulted in an eggless cake that had similar physicochemical properties, such as specific volume, texture, and specific gravity, to the control cakes. In addition, this eggless cake was more affordable compared with traditional cakes containing eggs (\$1.84/kg of batter vs. \$2.11/kg of batter). In terms of the conformations of macromolecules, the combination of SPI and 1% MDG also mimicked most of the structural properties of the gluteins in traditional cakes. The gliadin aggregates in R3 and control cakes were smaller in size and dominant in the range of 100–200 nm. In addition, these two cakes had glutenin thin layers of about 7 nm in height and networking structures with few, but large, pores. As the batter viscosity of R3 cake was significantly higher compared with that of the control cake, further improvement of the recipe is needed.

#### Conflict of interest statement

We declare that we do not have any commercial or associative interest that represents a conflict of interest in connection with this manuscript. We have no financial and personal relationships with other people or organisations that can inappropriately influence our work.

#### Acknowledgements

The authors acknowledge the financial support by Guangzhou Welbon Biological Technology Co., Ltd. (R-143-000-577-597).

#### Appendix A. Supplementary data

Supplementary data associated with this article can be found, in the online version, at <http://dx.doi.org/10.1016/j.foodchem.2017.02.132>.

#### References

- An, H., Liang, H., Liu, Z., Yang, H., Liu, Q., & Wang, H. (2011). Nano-structures of debranched potato starch obtained by isoamylolysis. *Journal of Food Science*, *76* (1), N11–14.
- Arozarena, I., Bertholo, H., Empis, J., Bunger, A., & Sousa, I. (2001). Study of the total replacement of egg by white lupine protein, emulsifiers and xanthan gum in yellow cakes. *European Food Research and Technology*, *213*(4), 312–316.
- Ashwini, A., Jyotsna, R., & Indrani, D. (2009). Effect of hydrocolloids and emulsifiers on the rheological, microstructural and quality characteristics of eggless cake. *Food Hydrocolloids*, *23*(3), 700–707.
- Belton, P. (1999). Mini review: on the elasticity of wheat gluten. *Journal of Cereal Science*, *29*(2), 103–107.
- Byler, D. M., & Susi, H. (1986). Examination of the secondary structure of proteins by deconvolved FTIR spectra. *Biopolymers*, *25*(3), 469–487.
- Chong, J. X., Lai, S., & Yang, H. (2015). Chitosan combined with calcium chloride impacts fresh-cut honeydew melon by stabilising nanostructures of sodium-carbonate-soluble pectin. *Food Control*, *53*, 195–205.
- Dong, F., Zhang, M., Tang, W.-W., & Wang, Y. (2015). Formation and mechanism of superhydrophobic/hydrophobic surfaces made from amphiphiles through droplet-mediated evaporation-induced self-assembly. *The Journal of Physical Chemistry B*, *119*(16), 5321–5327.
- Du, X., An, H., Liu, Z., Yang, H., & Wei, L. (2014). Probing starch–iodine interaction by atomic force microscopy. *Scanning*, *36*(4), 394–400.
- Feng, X., Fu, C., & Yang, H. (2017). Gelatin addition improves nutrient retention, texture and mass transfer of fish balls without altering their nanostructure during boiling. *LWT—Food Science and Technology*, *77*, 142–151.
- Feng, X., Ng, V. K., Mikš-Krajnc, M., & Yang, H. (2017). Effects of fish gelatin and tea polyphenol coating on the spoilage and degradation of myofibril in fish fillet during cold storage. *Food and Bioprocess Technology*, *10*(1), 89–102.
- Cómez, M., Ronda, F., Caballero, P. A., Blanco, C. A., & Rosell, C. M. (2007). Functionality of different hydrocolloids on the quality and shelf-life of yellow layer cakes. *Food Hydrocolloids*, *21*(2), 167–173.
- Ji, N., Li, X., Qiu, C., Li, G., Sun, Q., & Xiong, L. (2015). Effects of heat moisture treatment on the physicochemical properties of starch nanoparticles. *Carbohydrate Polymers*, *117*, 605–609.
- Jyotsna, R., Sai Manohar, R., Indrani, D., & Venkateswara Rao, G. (2007). Effect of whey protein concentrate on the rheological and baking properties of eggless cake. *International Journal of Food Properties*, *10*(3), 599–606.
- Kiosseoglou, V. (2003). Egg yolk protein gels and emulsions. *Current Opinion in Colloid & Interface Science*, *8*(4), 365–370.
- Kontogiorgos, V. (2011). Microstructure of hydrated gluten network. *Food Research International*, *44*(9), 2582–2586.
- Lagrain, B., Thewissen, B. G., Brijs, K., & Delcour, J. A. (2008). Mechanism of gliadin–glutenin cross-linking during hydrothermal treatment. *Food Chemistry*, *107*(2), 753–760.
- Liu, H., Chen, F., Lai, S., Tao, J., Yang, H., & Jiao, Z. (2017). Effects of calcium treatment and low temperature storage on cell wall polysaccharide nanostructures and quality of postharvest apricot (*Prunus armeniaca*). *Food Chemistry*, *225*, 87–97.
- Liu, H., Liang, R., Antoniou, J., Liu, F., Shoemaker, C. F., Li, Y., & Zhong, F. (2014). The effect of high moisture heat-acid treatment on the structure and digestion property of normal maize starch. *Food Chemistry*, *159*, 222–229.
- Liu, Q., Tan, C. S. C., Yang, H., & Wang, S. (2017). Treatment with low-concentration acidic electrolysed water combined with mild heat to sanitise fresh organic broccoli (*Brassica oleracea*). *LWT—Food Science and Technology*, *79*, 594–600.
- Liu, S., & Wang, Y. (2011). A review of the application of atomic force microscopy (AFM) in food science and technology. *Advances in Food and Nutrition Research*, *62*, 201–240.
- Lookhart, G., & Bean, S. (1995). Separation and characterization of wheat protein fractions by high-performance capillary electrophoresis. *Cereal Chemistry*, *72*(6), 527–532.
- Majzoobi, M., Ghiasi, F., Habibi, M., Hedayati, S., & Farahnaky, A. (2014). Influence of soy protein isolate on the quality of batter and sponge cake: Influence of soy protein isolate on sponge cake. *Journal of Food Processing and Preservation*, *38*(3), 1164–1170.
- Mao, L., Roos, Y. H., Biliaderis, C. G., & Miao, S. (2015). Food emulsions as delivery systems for flavor compounds – A review. *Critical Reviews in Food Science and Nutrition*. <http://dx.doi.org/10.1080/10408398.2015.1098586>.
- Miao, M., Jiang, B., Zhang, T., Jin, Z., & Mu, W. (2011). Impact of mild acid hydrolysis on structure and digestion properties of waxy maize starch. *Food Chemistry*, *126* (2), 506–513.

- Primo-Martín, C., van Nieuwenhuijzen, N. H., Hamer, R. J., & van Vliet, T. (2007). Crystallinity changes in wheat starch during the bread-making process: Starch crystallinity in the bread crust. *Journal of Cereal Science*, 45(2), 219–226.
- Rahmati, N. F., & Mazaheri Tehrani, M. (2014). Replacement of egg in cake: Effect of soy milk on quality and sensory characteristics. *Journal of Food Processing and Preservation*, 39(6), 574–582.
- Ratnayake, W. S., Geera, B., & Rybak, D. A. (2012). Effects of egg and egg replacers on yellow cake product quality. *Journal of Food Processing and Preservation*, 36(1), 21–29.
- Sahi, S. S., & Alava, J. M. (2003). Functionality of emulsifiers in sponge cake production. *Journal of the Science of Food and Agriculture*, 83(14), 1419–1429.
- Seabourn, B. W., Chung, O. K., Seib, P. A., & Mathewson, P. R. (2008). Determination of secondary structural changes in gluten proteins during mixing using fourier transform horizontal attenuated total reflectance spectroscopy. *Journal of Agricultural and Food Chemistry*, 56(11), 4236–4243.
- Sivam, A. S., Sun-Waterhouse, D., Perera, C. O., & Waterhouse, G. I. N. (2012). Exploring the interactions between blackcurrant polyphenols, pectin and wheat biopolymers in model breads; a FTIR and HPLC investigation. *Food Chemistry*, 131(3), 802–810.
- Sow, L. C., & Yang, H. (2015). Effects of salt and sugar addition on the physicochemical properties and nanostructure of fish gelatin. *Food Hydrocolloids*, 45, 72–82.
- Stone, H., & Sidel, J. (2004). *Sensory evaluation practices*. Sensory evaluation practices (3rd ed.). San Diego: Academic Press.
- Wang, P., Chen, H., Mohanad, B., Xu, L., Ning, Y., Xu, J., ... Xu, X. (2014). Effect of frozen storage on physico-chemistry of wheat gluten proteins: Studies on gluten-, glutenin- and gliadin-rich fractions. *Food Hydrocolloids*, 39, 187–194.
- Wang, Q., Li, Y., Sun, F., Li, X., Wang, P., Sun, J., ... He, G. (2015). Tannins improve dough mixing properties through affecting physicochemical and structural properties of wheat gluten proteins. *Food Research International*, 69, 64–71.
- Wilderjans, E., Luyts, A., Brijs, K., & Delcour, J. A. (2013). Ingredient functionality in batter type cake making. *Trends in Food Science & Technology*, 30(1), 6–15.
- Wilderjans, E., Pareyt, B., Goesaert, H., Brijs, K., & Delcour, J. A. (2008). The role of gluten in a pound cake system: A model approach based on gluten–starch blends. *Food Chemistry*, 110(4), 909–915.
- Xie, X., Cui, S. W., Li, W., & Tsao, R. (2008). Isolation and characterization of wheat bran starch. *Food Research International*, 41(9), 882–887.
- Xie, Y. R., & Hettiarachchy, N. S. (1998). Effect of xanthan gum on enhancing the foaming properties of soy protein isolate. *Journal of the American Oil Chemists' Society*, 75(6), 729–732.
- Xin, Y., Chen, F., Yang, H., Zhang, P., Deng, Y., & Yang, B. (2010). Morphology, profile and role of chelate-soluble pectin on tomato properties during ripening. *Food Chemistry*, 121(2), 372–380.
- Yang, H., Wu, Q., Ng, L. Y., & Wang, S. (2017). Effects of vacuum impregnation with calcium lactate and pectin methyltransferase on quality attributes and chelate-soluble pectin morphology of fresh-cut papayas. *Food and Bioprocess Technology*. <http://dx.doi.org/10.1007/s11947-017-1874-7>.